Postprint of: Szociński M., Darowicki K., Performance of organic coatings upon cyclic mechanical load, PROGRESS IN ORGANIC COATINGS, Vol. 146 (2020), 105718, DOI: 10.1016/j.porgcoat.2020.105718



# PERFORMANCE OF ORGANIC COATINGS UPON CYCLIC MECHANICAL LOAD

**M. Szociński*, K. Darowicki**

*Gdańsk University of Technology, Chemical Faculty,*
*Department of Electrochemistry, Corrosion and Materials Engineering,*
*11/12 G. Narutowicza Str., Gdańsk 80-233, POLAND*

## Abstract

A number of engineering structures fail due to the fatigue damage resulting from cyclic mechanical stress. However, as far as organic coatings are concerned this degradation factor remains underestimated. In the paper the authors propose a methodology combining global electrochemical impedance spectroscopy and local atomic force microscopy measurements for evaluation of coating resistance to an impact of repetitive mechanical stress. Typical epoxy coating designated for ship hull protection has been tested in as-received state as well as after pre-exposure to elevated temperature. Application of atomic force microscopy-based approach helped to reveal and spatially localize the spots of organic coating degradation onset. The mechanism and process of defect formation and propagation has been shown on a microscopic scale.

**Keywords:** organic coatings; fatigue damage; cyclic mechanical stress; electrochemical impedance spectroscopy; atomic force microscopy

## 1. Introduction

Protective and decorative function of organic coatings strongly depend on their mechanical properties. At each stage of the lifetime, from application through exploitation till degradation, coating are subjected to different types of mechanical stress and deformation [1-3]. One of the types of mechanical impact is cyclic stress of subcritical character. In this case the magnitude of stress associated with a single deformation cycle does not exceed yield strength of the material. Degradation arises due to a big number of repeating deformation cycles, which lead to stress accumulation. A fatigue damage is a result of such action. In practice, there is a number of objects and installations protected with organic coatings, which are subjected to cyclic mechanical stress – bridges and overpasses (stress associated with traffic), posts and masts (vibrations caused by wind), ship hulls and casings of machines (stress caused by engine operation), etc. [4,5].

*Corresponding author. Phone: +48 58 348-63-96 Fax: +48 58 347-10-92
E-mail: micszoci@pg.edu.pl

The problem of fatigue damage of coating due to cyclic stress becomes more serious with the progress of service, when the polymers are subjected to the processes of chemical degradation and physical ageing caused by the impact of environment. For instance, presence of oxygen or ultraviolet radiation can contribute to various photolytic reactions, leading to formation of free radicals and peroxides. This phenomenon can enhance disorganization and breakdown of internal structure of polymer material, hence causing an increase in coating brittleness [6-8]. Irreversible changes in the coating, being a result of ageing, increase its stiffness and thus susceptibility to failure upon mechanical stress. Cyclic mechanical stress also deteriorates performance of the multilayer coating systems affecting interlayer adhesion [9]. More detailed discussion on the mechanism of organic coating degradation upon cyclic mechanical stress has been presented in the paper of Darowicki and Szociński [8]. Nevertheless, the knowledge on fatigue damage of organic coatings caused by cyclic mechanical stress still seems to be incomplete, which is evidenced by relatively low number of papers on the subject. The fact that this factor remains underestimated is also evidenced by the lack of a standard test in this field.

Durability of organic coating subjected to alternating mechanical stress is determined by the weakest element of its structure. These sites becomes spots of stress accumulation and they constitute the nuclei of stress and defect propagation. That is why identification of these regions is of vital importance from the standpoint of understanding the coating behaviour upon mechanical stress influence. The knowledge about micro-discontinuities in coatings' structure is especially crucial for research and development entities and well as paint producers. Such information can be potential hints concerning the degradation mechanism and improvements that should be done in order to increase coating lifetime.

However, acquisition of the aforementioned information of local character calls for suitable measurement techniques. Majority of standard tests, such as adhesion, thickness, hardness or chemical resistance tests, despite their undisputable utility, are not local and do not provide a resolution of micro or nanometre order. Similarly electrochemical impedance spectroscopy, which for many years has been successfully applied to evaluation of the state and degradation progress of organic protective coatings [10-15] typically provides the results averaged over relatively large surface area of several centimetres order.

Accordingly, the authors of the paper decided to investigate a phenomenon of organic coatings degradation subjected to cyclic mechanical stress, compare durability of as-received and aged coating exposed to alternating stress and to identify the spots of degradation onset caused by mechanical factor. To achieve that classical global electrochemical impedance spectroscopy technique has been employed in tandem with a local technique, namely atomic force microscopy (AFM) approach

enabling measurement of local coating topography and local electrical properties. Recently, it was successfully employed to identification of local degradations spots in the coatings subjected to impact of electrolyte and UV radiation [16-18], coating behaviour at elevated temperatures [19] as well as investigation of zin-rich coatings [20]. Details of the technique have been presented elsewhere [21].

## 2. Experimental

The coating designated for the study was commercially available product Epinox77 from Teknos Co.. It is a high solid, two component epoxy primer dedicated to protection of ship's steel hulls, steel constructions operating in sea, coastal and industrial environment as well as to steel and cast iron constructions exposed to destructive mechanical factors [22]. The system under investigation consisted of epoxy coating on 0.5 mm thick S235JR steel substrate [23]. The paint was applied in two layers using air spray technique. The average thickness was equal to 120.3 ± 7.2 μm. The samples were seasoned for 1 week in the laboratory prior to the investigation.

Steel substrate was in the form of an isosceles triangle to provide uniform stress distribution all over the specimen surface [24]. The characteristic dimensions are provided in Fig. 1. The substrates were prepared by grinding with abrasive paper of the 180-2000 gradation and degreased with acetone.

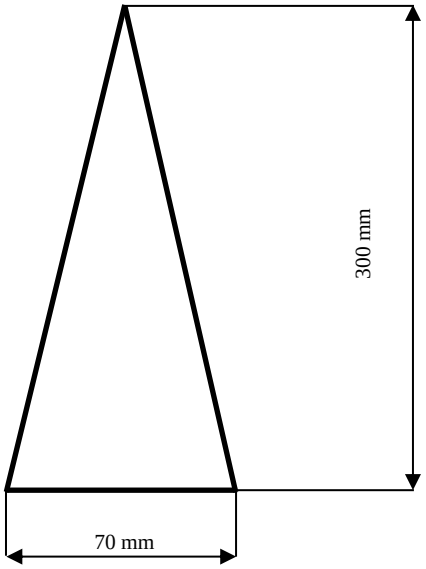


Fig. 1. Characteristic dimensions of the steel substrate.

One set of samples was tested against cyclic mechanical stress in as-received form. The second one was exposed to the conditions enhancing coating degradation – 3 months exposure at 70°C to induce physical ageing of polymer – and then subjected to mechanical cycles. A control sample was also included in the test. Each type of the investigated sample (non-aged, aged and control one) was prepared in four replicates in order to ensure representativeness of the results.

All the specimens were subjected to bend/ release cycles with the frequency f=1 Hz simulating fatigue damage. The applied force provided maintenance of the substrate within elastic deformation region. Since the maximum bending stress of the steel utilized in the research is 145MPa [23], the dimensions of the substrate and its deflection during cycling were adjusted to attain maximum 100MPa. In actual service conditions steel structures are not allowed to reach their mechanical limits, so the value of 100MPa corresponded to such situation, even with some extra safety margin. Accordingly, the bending stress of a substrate was the criterion of choice. The cycles were accomplished with a self-assembled fatigue test machine, which had been presented in details in [9]. The total number of bend/ release cycles imposed was equal to 350 000.

The state of the coatings was evaluated using electrochemical impedance spectroscopy technique. Impedance spectra were recorded regularly after fixed number of bend/ release cycles using Schlumberger SI 1255 Frequency Response Analyser coupled to a high input impedance buffer ATLAS 9181. The spectra were collected in the frequency range 1 MHz – 1 mHz and the amplitude of perturbation signal was equal to 30 mV peak-to-peak. There was no dc bias imposed and the measurements were performed at an open circuit potential. The investigation was carried out upon immersion in 3% NaCl in a two-electrode system. Metal substrate was a working electrode and platinum mesh served as a counter electrode. The area exposed to examination was 10.2 $cm^2$. The working area of the sample was delimited by positioning a 3.6-diameter PVC cylinder on the surface, in the central part of the triangular substrate. After a given series of the bend/release cycles, the cylinder with an O-ring seal at its bottom, in order to provide leak tightness, was attached with a dedicated clamp. This arrangement allowed removal of the cylinder before the next series of the fatigue cycles. Obtained impedance spectra were modelled with the equivalent circuits presented in Fig. 2. Electrical parameters of the coatings were acquired using EC-Lab software [25]. Due to non-ideal capacitive behaviour of the coatings, especially at the later stages of the experiment, an ideal capacitor describing coating capacitance in the electrical equivalent circuit was substituted with a constant phase element (CPE). Impedance of this element can be described as follows:

$$Z = \frac{1}{Q(j\omega)^n} \quad (1)$$

where:

Q and n are the parameters of CPE and ω stands for the angular frequency. The n parameter can take the value from zero to unity. If n=1, Q represents ideal capacitance. When n=0, then Q describes pure resistor. Accordingly, it can be accepted that the n parameter describes a degree of deviation of the modelled system from ideal capacitive behaviour. Many real systems, including organic coatings on metallic substrates, reveal surface and bulk inhomogeneity resulting from non-uniform composition, presence of defects introduced at the production, application or exploitation stage, etc. [26,27]. These factors cause non-uniform resistive-capacitive behaviour over the specimen surface manifested by various durability with respect to degradation factors or electrolyte uptake. That is why precise modelling of those materials requires substitution of an ideal capacitor with the CPE, which accounts for the aforementioned local heterogeneity, and the n parameter can be used as an indicator of deviation from ideal capacitor and thus of an increase in material's heterogeneity.



a)

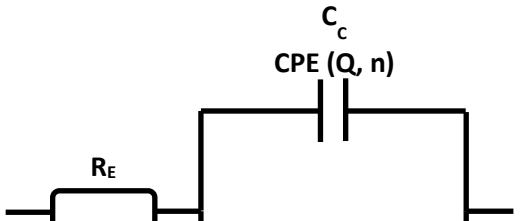

b)

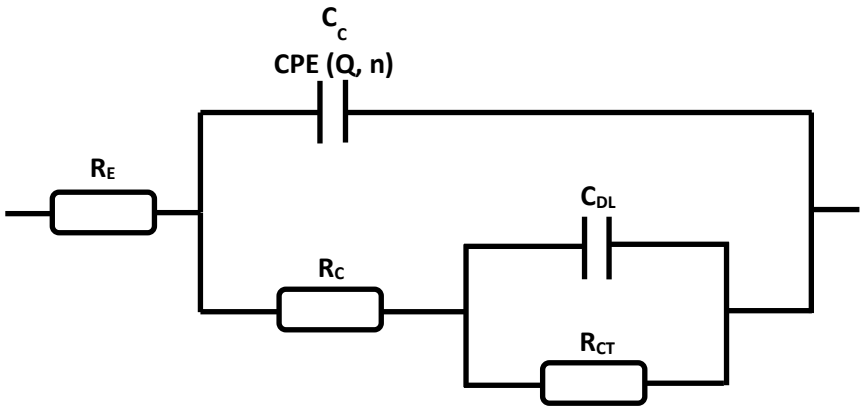


Fig. 2. Equivalent circuits used to model the spectra recorded: (a) for intact coating situation, (b) for defected coating situation, where: $R_E$ – electrolyte resistance, $R_C$ – coating resistance, $R_{CT}$ – charge transfer resistance, $C_C$ – coating capacitance, $C_{DL}$ – double layer capacitance.

Atomic force microscopy measurements were executed with the SPM Ntegra Aura system by NT-MDT Co.. The scans were performed in dry conditions, without immersion in an electrolyte. The maximum scan area was 8100μm$^2$(90μmx90μm). Scanning by tip mode was employed. Scanning frequency was equal to 1Hz. All the images were collected for the set point providing 6μN contact force. The parameters of a diamond coated AFM tip used are shown in Table 1. Recording of the images, their processing and analysis involved the Nova software by NT-MDT Co..

Table 1. Parameters of the tip DCP20 by NT-MDT utilized in the investigations.

| Chip size [mm] | Tip height [μm] | Tip curvature radius [nm] | Tip side coating | Cantilever length [μm] | Cantilever width [μm] | Cantilever thickness [μm] | Resonant frequency [kHz] | Force constant [N/m] |
|---|---|---|---|---|---|---|---|---|
| 3.6x1.6x0.4 | 10-15 | 35 | diamond 70nm | 90 | 60 | 1.7-2.3 | 350-800 | 40-110 |

Local impedance spectroscopy was performed in the stationary regime with the AFM tip positioned at selected localization of interest. The measurement set-up was comprised of the Parstat 2236 workstation configured in two-terminal measurement mode. One terminal was connected to the metallic substrate, the second one was in contact with the conductive layer of the AFM probe by means of a dedicated holder. Local impedance spectra were recorded in the frequency range between 0.1MHz and 1Hz with 30 points per frequency decade. Amplitude of perturbation voltage was 100mV RMS. The measurements were carried out in dry conditions, without immersion in electrolyte.

Spreading resistance measurements were performed for a bias voltage of 20mV applied between the AFM tip and the coated metal substrate. Corresponding dc current maps were collected during scanning at a rate of 1Hz.

## 3. **Results and discussion**

The investigation revealed differences in behaviour of the coatings subjected to examination. Fig. 3 presents the exemplary impedance spectra in Bode format recorded for the epoxy coating, which was subjected to cyclic mechanical stress in as-received state, without any pre-exposure. There is little difference between the initial spectrum and the one obtained after 350 000 bend/ release cycles. The coating still provides excellent barrier properties against corrosion agents. The electrical parameters of the coating (its resistance $R_c$, the parameters $Q$ and $n$ of the CPE modelling coating capacitance) change only slightly with the number of the cycles – see Figs 6 a b c. Their values and course of changes are similar to those obtained for a control sample. Fig. 4 illustrates the exemplary impedance spectra in Bode format for the control sample of epoxy coating, not subjected to cyclic mechanical stress but immersed in 3% NaCl solution for 360 hours. It is a period of time equivalent to the total immersion time experienced by the samples during impedance tests executed after successive number of the mechanical cycles. In the case of stressed as well as control samples, the coatings exhibit good dielectric properties maintaining the resistance of $10^{11}$ $\Omega cm^2$ order. Coating capacitance exhibits slightly increasing trend, which is an evidence of limited electrolyte uptake by the coatings. The $n$ parameter of the CPE element also reveals only small decrease during the entire test duration suggesting preservation of substantial homogeneity of the protective films.

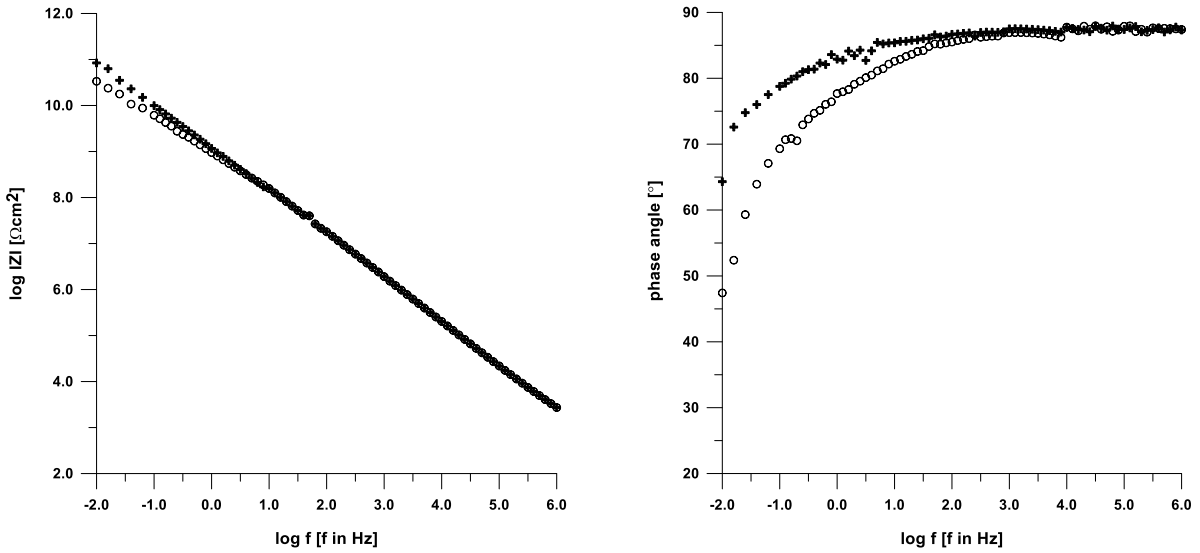


Fig. 3. Exemplary impedance spectra in Bode format for epoxy coating subjected to cyclic mechanical stress in as-received state (+ initial spectrum, ○ after 350 000 mechanical cycles).

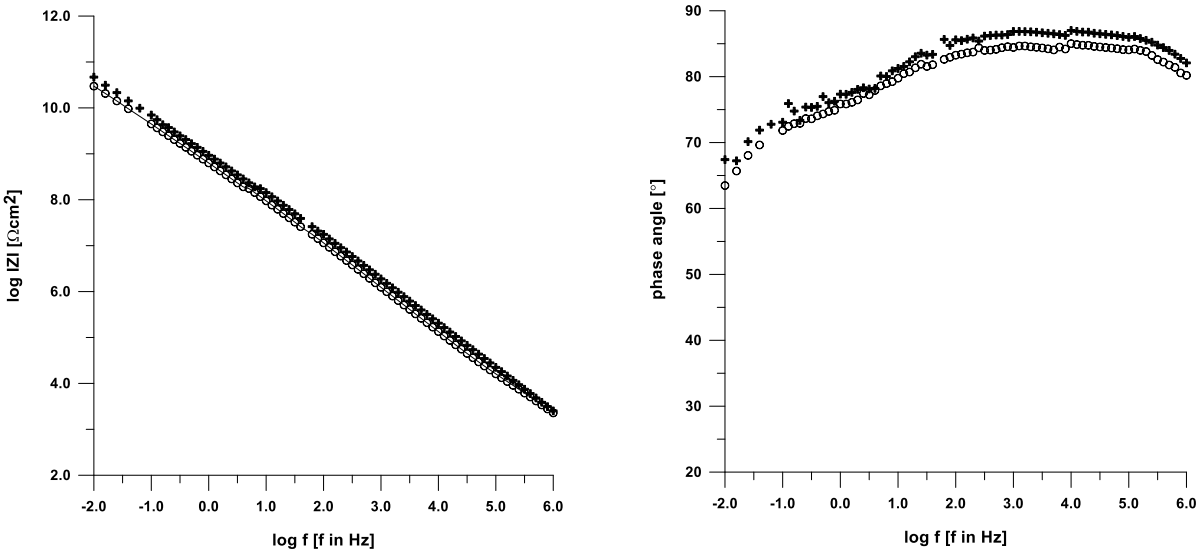


Fig. 4. Exemplary impedance spectra in Bode format for control sample of epoxy coating, not subjected to cyclic mechanical stress but immersed in 3% NaCl solution (+ initial spectrum, ○ after 360 hours of immersion).

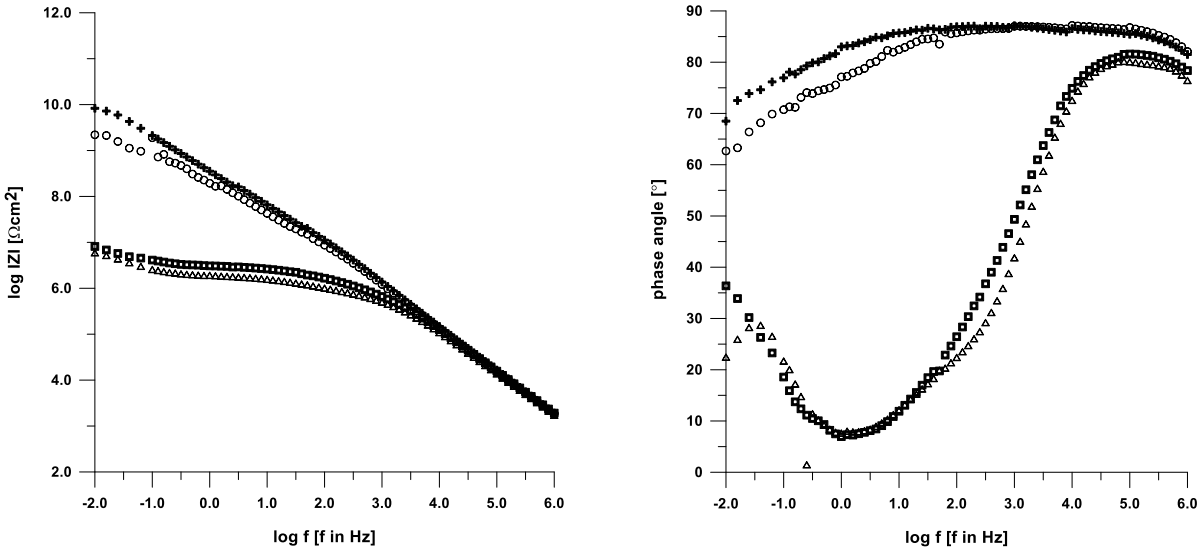


Fig. 5. Exemplary impedance spectra in Bode format for epoxy coating subjected to cyclic mechanical stress after pre-exposure at 70°C for 3 months (+ initial spectrum, ○ after 146 000 mechanical cycles, □ after 167 000 cycles, Δ after 210 000 cycles).

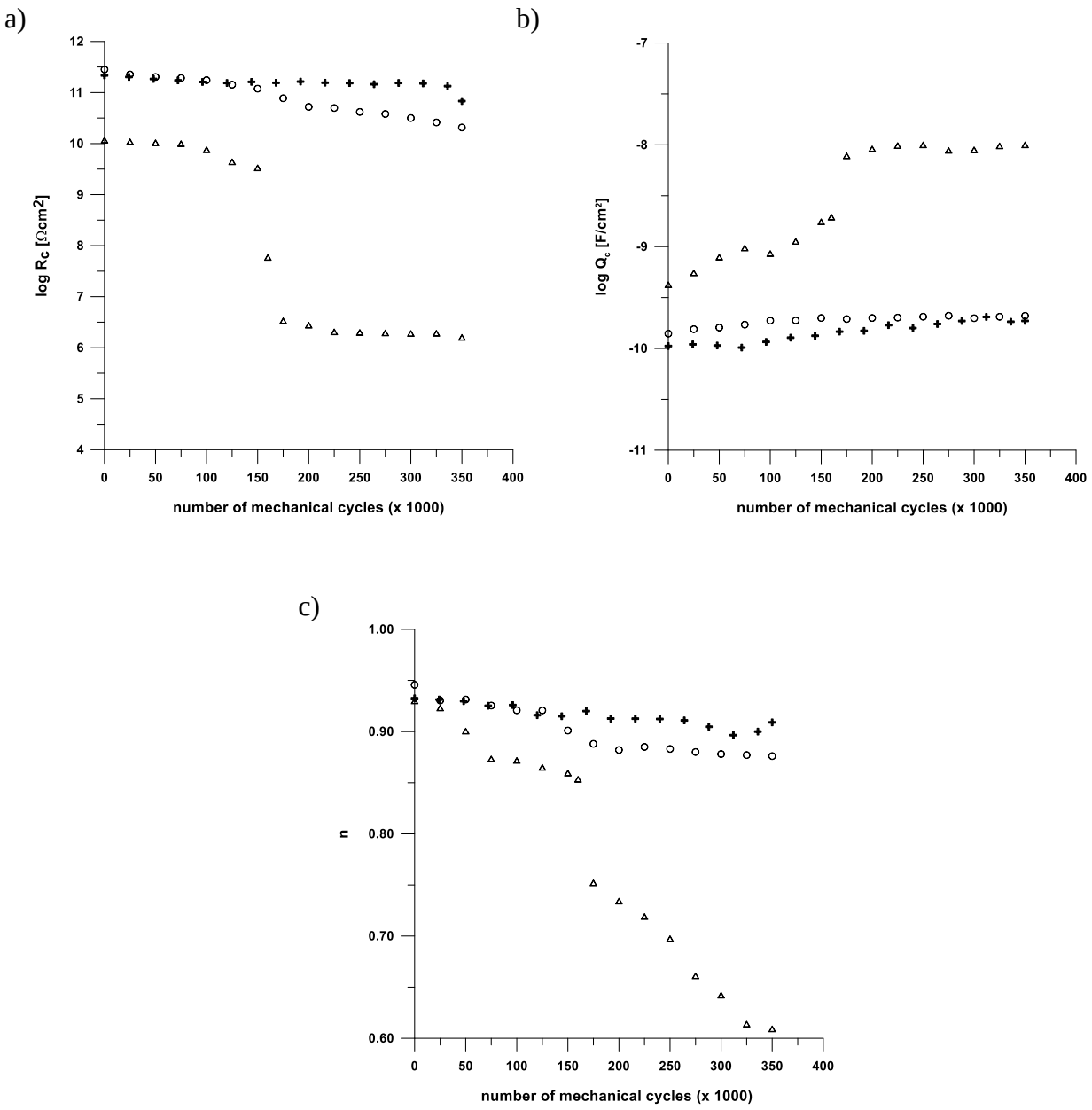


Fig. 6. Evolution of coatings electrical parameters during the test: a) coating resistance, b) *Q* parameter of CPE modelling coating capacitance, c) *n* parameter of CPE modelling coating capacitance (+ control sample, ○ sample subjected to mechanical cycles in as-received state, Δ sample subjected to mechanical cycles after pre-exposure at 70°C for 3 months).

Fig. 7a depicts an exemplary AFM topographical image of the epoxy coating, which was subjected to 350 000 cycles in as received state. There are no signs of defects presence in the protective film as the image presents typical coating surface with some hills and valleys, stemming probably from application quality. The maximum difference in profile height does not exceed 2.5μm.

Lack of defects is confirmed by the local dc current map corresponding to the aforementioned topographical image (Fig. 7b). The current recorded is low – below ca. 4.5pA – and uniform in magnitude over the entire examined surface, indicating lack of through-the-coating defects.

a) b)

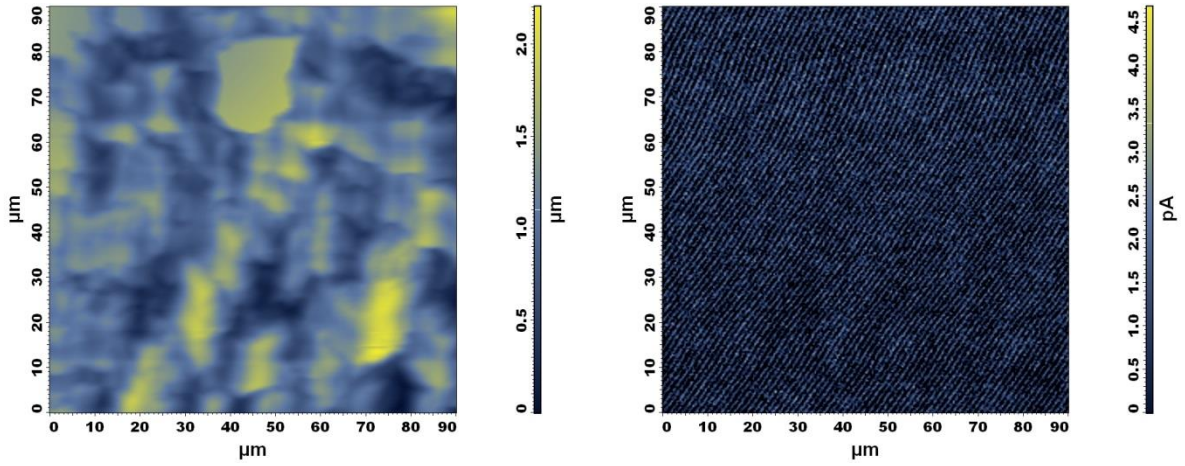


Fig. 7. Exemplary AFM images of epoxy coating subjected to 350 000 mechanical cycles in as-received state: a) topographical image, b) local dc current map.

The situation is different in case of the pre-exposed sample. Its increased vulnerability to fatigue failure upon mechanical cycling becomes evident in Fig. 5. Three months at 70°C made the coating more prone to degradation due to cyclic mechanical stress. The exposure did not result in immediate loss in protective properties of the epoxy coating as the initial spectrum illustrates impedance of $10^{10}\,\Omega cm^2$ order. During the first couple of cyclic stress series the barrier effect was maintained. Significant deterioration of the dielectric properties occurred beyond 146 000 cycles. Till that moment an incubation period could be distinguished – the coating electrical parameters (Fig. 6) remained at approximately constant level and the coating was able to withstand repetitive mechanical stress. After a threshold value had been attained, quite rapid departure from the previous parameters took place. The coating resistance reached the level of $10^6\,\Omega cm^2$, which is believed to be the one separating good barrier coating from the film that should be discarded from further exploitation. Enhanced electrolyte uptake accounts for an increase in the coating capacitance by about one order of magnitude. There is also a sudden drop in the *n* parameter of CPE showing deterioration of coating homogeneity. Moreover, the impedance spectra clearly show presence of the second, low-

frequency time constant corresponding to an electrochemical reaction on the metal substrate, thus the coating does not constitute a barrier to corrosion agents at this stage of the experiment.

Interesting information is acquired via the local measurements performed using the atomic force microscopy-based approach. Fig. 8a illustrates a topographical image of the coating subjected to 50 000 mechanical cycles after 3-month ageing at elevated temperature. As opposed to the non-aged sample, there can be seen some tiny cracks running randomly over the coating surface. The maximum difference in profile height increased to ca. 5.5µm. It can be supposed that such image of the surface is a response to fatigue cycles and the cracks can be potential defect sites. In order to confirm this supposition, a corresponding local dc current map was collected (Fig. 8b). However, it did not reveal any increased conductivity of these regions, indicating that the coating was still holiday-free at this stage of exposure. The magnitude of dc current was uniform over the investigated surface and was lower than ca. 12pA.

a) b)

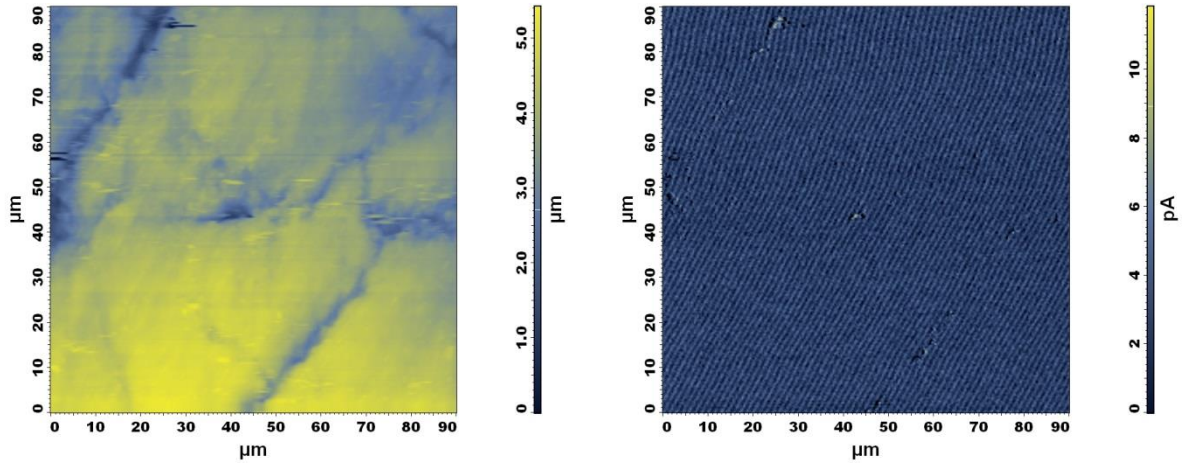


Fig. 8. Exemplary AFM images of epoxy coating subjected to 50 000 mechanical cycles after pre-exposure at 70°C for 3 months: a) topographical image, b) local dc current map.

Radical change took place beyond 146 000 mechanical cycles. Fig. 9a presents a topographical image of the epoxy coating subjected to 167 000 mechanical cycles after pre-exposure at 70°C for 3 months. Much broader and well-resolved cracks are clearly visible on the analysed surface. It is evident that previously identified cracks enlarged significantly and it is highly probable that they became serious coating defects. In order to verify if these really constitute through-the-coating defects, a local dc current map was acquired (Fig. 9b). In the locations corresponding to most of the cracks there is a

significant increase in current (about three orders of magnitude higher as compared to the previous situation), confirming direct access of corrosive agents to the metallic substrate. Further confirmation of the presence of through-the-coating defects is provided by a comparison of the local impedance spectra recorded for the AFM tip positioned inside the crack (Fig. 10a) and outside it, on intact coating fragment (Fig. 10b). The impedance inside the crack is more than 3 orders of magnitude lower than on the intact protective film. It should be emphasized that this degradation had discrete and local character. Visual observation, which was performed after each series of applied mechanical cycles, did not reveal any macroscopic changes in the coating surface appearance. Accordingly, this cyclic mechanical stress impact could be detected only with such tools as electrochemical impedance spectroscopy and atomic force microscopy.

a) b)

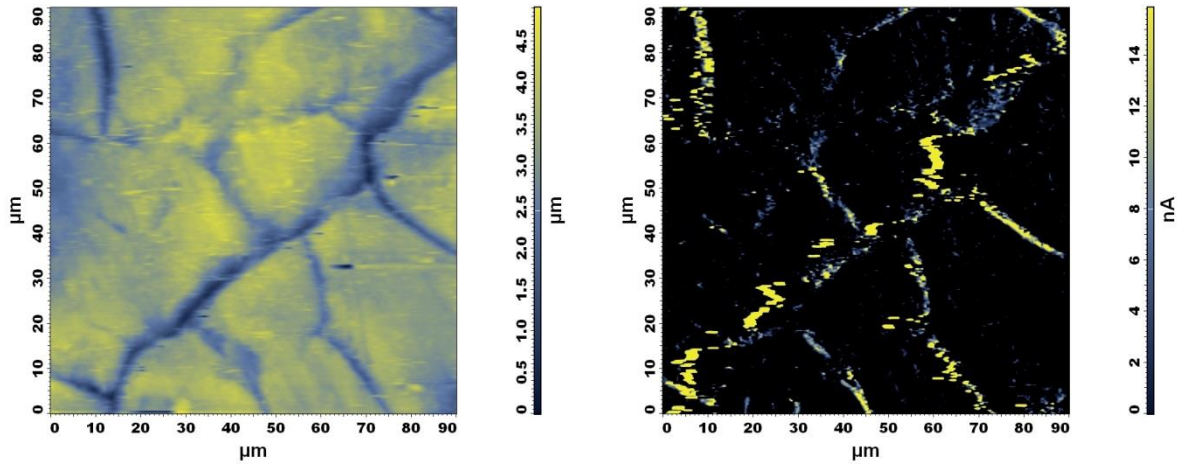


Fig. 9. Exemplary AFM images of epoxy coating subjected to 167 000 mechanical cycles after pre-exposure at 70°C for 3 months: a) topographical image, b) local dc current map.

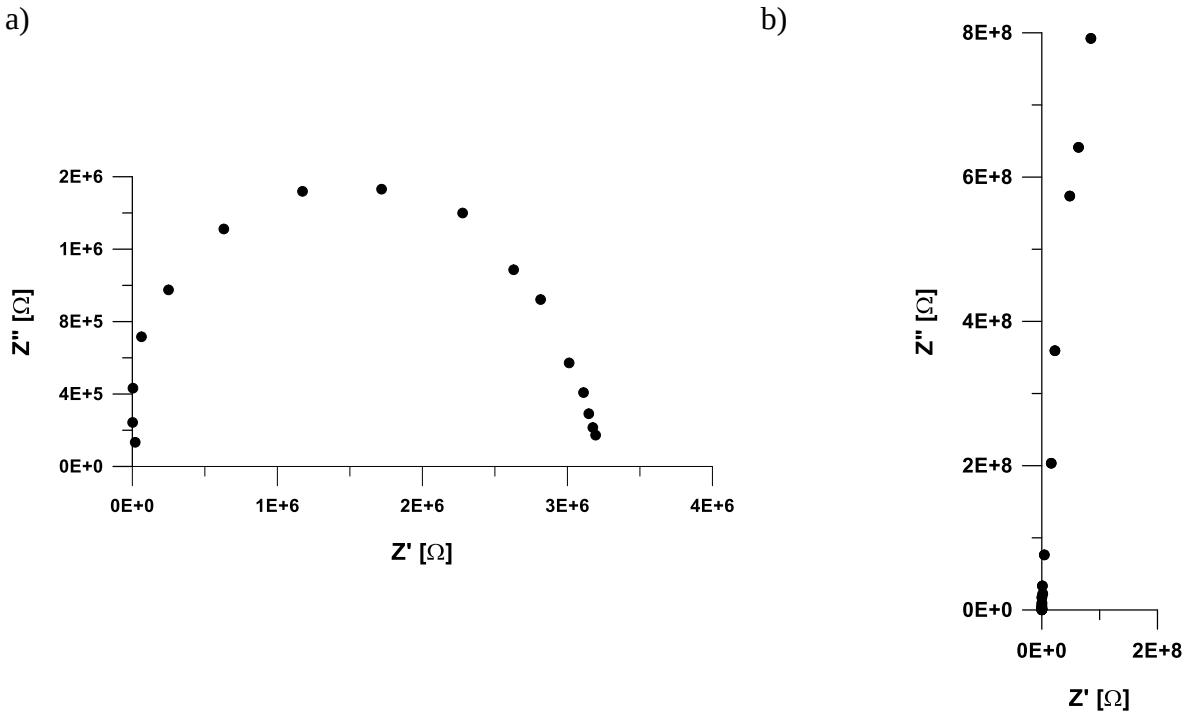


Fig. 10. Local impedance spectra of epoxy coating subjected to 167 000 mechanical cycles after pre-exposure at 70°C for 3 months: a) spectrum collected inside a crack in the coating, b) spectrum collected outside a crack, on intact coating region.

Summing up, the investigation performed proved that the fatigue effect in organic coatings originating from cyclic mechanical stress deserves serious attention. The problem becomes especially pronounced for aged coatings. The new system, in as-received state occurred to be flexible enough to resist the stress, so it performed much better during the test. However, majority of coatings experience ageing during service. It turned out that such factor as elevated temperature, frequent in the case of outdoor exposure, made the coating material more vulnerable to mechanical fatigue. In this way, already after much shorter service, the coating becomes susceptible to repetitive mechanical stress and undergoes accelerated, premature damage. What is more, proposed methodology of local measurements based on atomic force microscopy allowed identification and spatial localization of degradation precursor sites formed in the pre-exposed coating. Local electrical measurements made it possible to reveal that at the beginning these regions were not conductive, so the coating was still a barrier for corrosive agents. However, after application of bigger number of the mechanical cycles they became through-the-coating defects manifesting increased electrical activity.

## 4. **Conclusions**

The investigation on cyclic mechanical stress impact on epoxy coatings on steel substrates allows for the following final statements:

1. Cyclic mechanical stress is an important factor contributing to accelerated, premature degradation of the coatings.
2. Detrimental effect of repetitive stress becomes significant for aged coatings with the structure weakened by an exposure to a degradation factor, in this particular case elevated temperature.
3. The impact of cyclic stress is stronger while accompanied by other degradation factor, which suggests a synergistic effect.
4. Electrochemical impedance spectroscopy occurred to be a well-suited tool to follow the epoxy coating performance upon cyclic mechanical load.
5. More detailed insight into the coating fatigue degradation, inaccessible via classical global impedance measurement, was provided by the proposed approach based on atomic force microscopy.
6. Acquisition of local topographical and electrical AFM images allowed identification and spatial localization of the places responsible for coating degradation onset.
7. These were the local electrical characteristics (local dc current maps and local impedance spectra), which uncovered some preferential spots of coating degradation, although at the initial stage of exposure to the mechanical cycles they had still provided a barrier against corrosive agents. Bigger number of the mechanical stress cycles converted them into through-the-coating defects deciding about the loss of coatings protective properties.



## 5. Data availability

The raw/processed data required to reproduce these findings cannot be shared at this time as the data also forms part of an ongoing study.

## 6. References


[1] A. F. Abdelkader, J. R. White, Comparison of internal stresses in coatings cured on rigid substrates and on unrestrained thin substrates, Prog. Org. Coat. 44 (2002) 121-129.

[2] D. G. Weldon, Failure Analysis of Paints and Coatings, John Willey & Sons Ltd., New York, 2002.

[3] A. C. Bastos, A. M. Simoes, Effect of uniaxial strain on the protective properties of coil-coatings, Prog. Org. Coat. 46 (2003) 220-227.

[4] Z. X. Li, T. H. T. Chan, J. M. Ko, Fatigue analysis and life prediction of bridges with structural health monitoring data - Part I: methodology and strategy, Int. J Fatigue 23 (2001) 45-53.

[5] L. B. R. Robles, M. A. Buelta, E. Goncalves, G. F. M. Souza, A method for the evaluation of the fatigue operational life of submarine pressure hulls, Int. J Fatigue 22 (2000) 41-52.

[6] R. Lambourne, Paint and Surface Coatings: Theory and Practice, John Wiley & Sons Ltd., New York, 1987.

[7] P. A. Schweitzer, Mechanical and Corrosion-Resistant Properties of Plastics and Elastomers, Marcel Dekker Inc., New York, 2000.

[8] K. Darowicki, M. Szociński, Evaluating the performance of organic coatings under mechanical stress using electrochemical impedance spectroscopy, J Solid State Electrochem. 8 (6) (2004) 346-351.

[9] A. Miszczyk, M. Szociński, K. Darowicki, Interlayer defect evolution in an coating system on steel under hydromechanical loading, J. Appl. Electrochem. 37 (3) (2007) 353-358.

[10] F. Mansfeld, L. T. Han, C. C. Lee, G. Zhang, Evaluation of corrosion protection by polymer coatings using electrochemical impedance spectroscopy and noise analysis, Electrochim. Acta 43 (1998) 2933-2945.

[11] J. M. Hu, J. Q. Zhang, C. N. Cao, Determination of water uptake and diffusion of $Cl^-$ ion in epoxy primer on aluminium alloys in NaCl solution by electrochemical impedance spectroscopy, Prog. Org. Coat. 46 (2003) 273-279.

[12] S. Rossi, F. Deflorian, L. Fontanari, A. Cambruzzi, P. L. Bonora, Electrochemical measurements to evaluate the damage due to abrasion on organic protective system, Prog. Org. Coat. 52 (2005) 288-297.

[13] B. R. Hinderliter, S. G. Croll, D. E. Tallman, Q. Su, G. P. Bierwagen, Interpretation of EIS data from accelerated exposure of coated metals based on modeling of coating physical properties, Electrochim. Acta 51 (2006) 4505-4515.
[14] C. G. Oliveira, M. G. S. Ferreira, Ranking high-quality paint systems using EIS. Part I: intact coatings, Corros. Sci. 45 (2003) 123-138.
[15] C. G. Oliveira, M. G. S. Ferreira, Ranking high-quality paint systems using EIS. Part II: defective coatings, Corros. Sci. 45 (2003) 139-147.
[16] M. Szociński, K. Darowicki, K. Schaefer, Identification and localization of organic coating degradation onset by impedance imaging, Polym. Degrad. Stabil. 95 (2010) 960-964.
[17] M. Szociński, K. Darowicki, Local impedance spectra of organic coatings, Polym. Degrad. Stabil. 98 (2013) 261-265.
[18] M. Szociński, K. Darowicki, K. Schaefer, Application of impedance imaging to evaluation of organic coating degradation at a local scale, J Coat. Tech. Res. 10 (1) (2013) 65-72.
[19] M. Szociński, K. Darowicki, Local properties of organic coatings close to glass transition temperature, Prog. Org. Coat. 77 (2014) 2007-2011.
[20] M. Szociński, K. Darowicki, Performance of zinc-rich coatings evaluated using AFM-based electrical properties imaging, Prog. Org. Coat. 96 (2016) 58-64.
[21] K. Darowicki, M. Szociński, A. Zieliński, Assessment of organic coating degradation via local impedance imaging, Electrochim. Acta 55 (2010) 3741-3748.
[22] Epinox 77 epoxy primer datasheet.
https://www.teknos.com/document/tds/en_71030-00_4.pdf (accessed 7 April 2020).
[23] The European Structural Steel Standard EN 10025:2004, Part 2 – Technical delivery conditions for non-alloy structural steels.
[24] R. L. Brockenbrough, F. S. Merritt (Eds.), Structural Steel Designer's Handbook, third ed., McGraw-Hill Inc., 1999.
[25] EC-Lab Software User's Manual, BioLogic Science Instruments, 2014.
[26] G. Grundmeier, K. M. Juttner, M. Stratmann, Novel Electrochemical Techniques in Corrosion Research in: Materials Science and Technology. A Comprehensive Treatment, ed. by R. W. Cahn, P. Haasen, E. J. Kramer, Corrosion and Environmental Degradation Vol. I, Wiley-VCH Verlag GmbH, Weinheim, 2000.
[27] I. Dehri, M. Erbil, The effect of relative humidity on the atmospheric corrosion of defective organic coating materials: an EIS study with a new approach, Corros. Sci. 42 (2000) 969-978.

## Figure captions

Fig. 1. Characteristic dimensions of the steel substrate.

Fig. 2. Equivalent circuits used to model the spectra recorded: (a) for intact coating situation, (b) for defected coating situation, where: $R_E$ – electrolyte resistance, $R_C$ – coating resistance, $R_{CT}$ – charge transfer resistance, $C_C$ – coating capacitance, $C_{DL}$ – double layer capacitance.

Fig. 3. Exemplary impedance spectra in Bode format for epoxy coating subjected to cyclic mechanical stress in as-received state (+ initial spectrum, ○ after 350 000 mechanical cycles).

Fig. 4. Exemplary impedance spectra in Bode format for control sample of epoxy coating, not subjected to cyclic mechanical stress but immersed in 3% NaCl solution (+ initial spectrum, ○ after 360 hours of immersion).

Fig. 5. Exemplary impedance spectra in Bode format for epoxy coating subjected to cyclic mechanical stress after pre-exposure at 70°C for 3 months (+ initial spectrum, ○ after 146 000 mechanical cycles, □ after 167 000 cycles, Δ after 210 000 cycles).

Fig. 6. Evolution of coatings electrical parameters during the test: a) coating resistance, b) *Q* parameter of CPE modelling coating capacitance, c) *n* parameter of CPE modelling coating capacitance (+ control sample, ○ sample subjected to mechanical cycles in as-received state, Δ sample subjected to mechanical cycles after pre-exposure at 70°C for 3 months).

Fig. 7. Exemplary AFM images of epoxy coating subjected to 350 000 mechanical cycles in as-received state: a) topographical image, b) local dc current map.

Fig. 8. Exemplary AFM images of epoxy coating subjected to 50 000 mechanical cycles after pre-exposure at 70°C for 3 months: a) topographical image, b) local dc current map.

Fig. 9. Exemplary AFM images of epoxy coating subjected to 167 000 mechanical cycles after pre-exposure at 70°C for 3 months: a) topographical image, b) local dc current map.

Fig. 10. Local impedance spectra of epoxy coating subjected to 167 000 mechanical cycles after pre-exposure at 70°C for 3 months: a) spectrum collected inside a crack in the coating, b) spectrum collected outside a crack, on intact coating region.

## List of tables